Journal of Alloys and Compounds 619 (2015) 311–318

Contents lists available at ScienceDirect

Journal of Alloys and Compounds

journal homepage: www.elsevier.com/locate/jalcom

Amorphous phase formation in Fe–Ag-based immiscible alloys

Takeshi Nagase [a,b,*], Masanori Suzuki [b], Toshihiko Tanaka [b]

[a] Research Center for Ultra-High Voltage Electron Microscopy, Osaka University, 7-1 Mihogaoka, Ibaraki, Osaka 567-0047, Japan
[b] Division of Materials and Manufacturing Science, Graduate School of Engineering, Osaka University, 2-1 Yamada-Oka, Suita, Osaka 565-0871, Japan

ARTICLE INFO

Article history:
Received 3 July 2014
Received in revised form 14 August 2014
Accepted 26 August 2014
Available online 6 September 2014

Keywords:
Amorphous materials
Rapid-solidification
Electron microscopy

ABSTRACT

The formation of an amorphous phase was identified in Fe–Ag-based quaternary immiscible alloys of (Fe–M–B)–Ag, where M = Si, Zr, Nb. A macroscopically phase-separated melt-spun ribbon formed in the (Fe–Si–B)–Ag alloy was found to be composed of an *fcc*-Ag crystalline phase and an Fe–Si–B-based amorphous phase, a microstructure that is significantly different from that formed in an (Fe–Si–B)–Cu alloy system. An emulsion-type structure cannot be seen in the (Fe–Si–B)–Ag alloy.

1. Introduction

Two-phase amorphous alloys, representing a new type of immiscible metallic materials, have recently been developed in a number of different immiscible alloys [1–4]. The formation of the two amorphous phases derives from the positive heat of mixing between the two major elements, as well as from the high glass-forming ability (GFA) of the separated liquids. Binary Fe–Cu and Fe–Ag alloys are particularly well known as typical alloy systems that exhibit liquid-phase separation, albeit with a significant difference in the separation behavior of the liquid phases [5–8]. For instance, Fe–Cu alloys typically have a flat liquidus line in their thermal equilibrium phase diagram [5] and a metastable liquid miscibility below the liquidus [6]. In contrast, the phase diagram of the Fe–Ag alloy system (Fig. 1) shows both a Fe-rich and Ag-rich liquids [7,8], with no single liquid phase being evident. With regards to Fe–Cu-based alloys, there have as yet been no reports pertaining to the formation of a two-phase metallic amorphous phase, although the simultaneous occurrence of liquid phase separation and Fe-based amorphous phase formation has been reported in various Fe–Cu-based alloy systems [9–22].

The difference in liquid phase separation behavior between the Fe–Cu and Fe–Ag alloy systems implies a difference in the amorphous phase formation behavior and a rapidly solidified structure. However, to the best of our knowledge, only limited information concerning amorphous phase formation in Fe–Ag-based immiscible alloys has been reported to date [23]. In the present study, rapidly solidified quaternary Fe–M–B–Ag (M = Si, Zr, B) alloys were developed and investigated, with a focus on amorphous phase formation and the final microstructure. These particular alloy systems were selected on the combined basis of the amorphous phase-forming system of Fe–M–B (liquid stabilizing system) and the Fe–Ag liquid phase separation system (liquid destabilizing system).

2. Theoretical background

Combination maps showing the heat of mixing (ΔH_{mix}) for binary atomic pairs of constituent elements and the predicted quaternary phase diagrams [22], both of which are readily available, are valuable tools in the design of Fe–Ag-based immiscible alloys with liquid phase separation. As such, they were used in this study to predict Fe–Ag-based alloys that would exhibit liquid phase separation and amorphous phase formation simultaneously. The results for the quaternary (Fe–M–B)–Ag (M = Si, Zr, Nb) alloys are shown in Fig. 2, wherein the ternary Fe–Si–B, Fe–Zr–B, and Fe–Nb–B alloy systems are all well known to exhibit high glass-forming ability (GFA) [24]. The combination map of ΔH_{mix} for the binary atomic pairs of constituent elements (left side of Fig. 2) is based on previously published data [25], whereas the quaternary phase diagrams at (right side of Fig. 2) were constructed by the Materials Project based on first-principles calculations [26–29].

Among the Fe–Si–B–Ag (Fig. 2a), Fe–Zr–B–Ag (Fig. 2b), and Fe–Nb–B–Ag (Fig. 2c) systems, it is the latter that most closely matches a typical alloy system that exhibits simultaneous liquid phase separation and amorphous phase formation. In the

* Corresponding author at: Research Center for Ultra-High Voltage Electron Microscopy, Osaka University, 7-1 Mihogaoka, Ibaraki, Osaka 567-0047, Japan. Tel.: +81 6 6879 7941; fax: +81 6 6879 7942.
E-mail address: t-nagase@uhvem.osaka-u.ac.jp (T. Nagase).

http://dx.doi.org/10.1016/j.jallcom.2014.08.212
0925-8388/

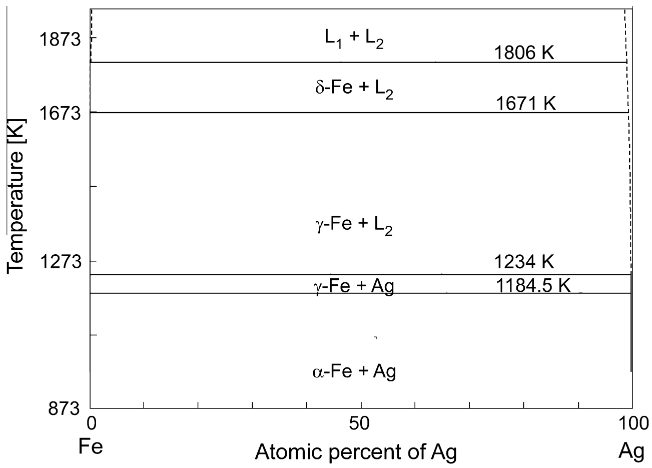

Fig. 1. Binary phase diagram of the Fe–Ag alloy system [7].

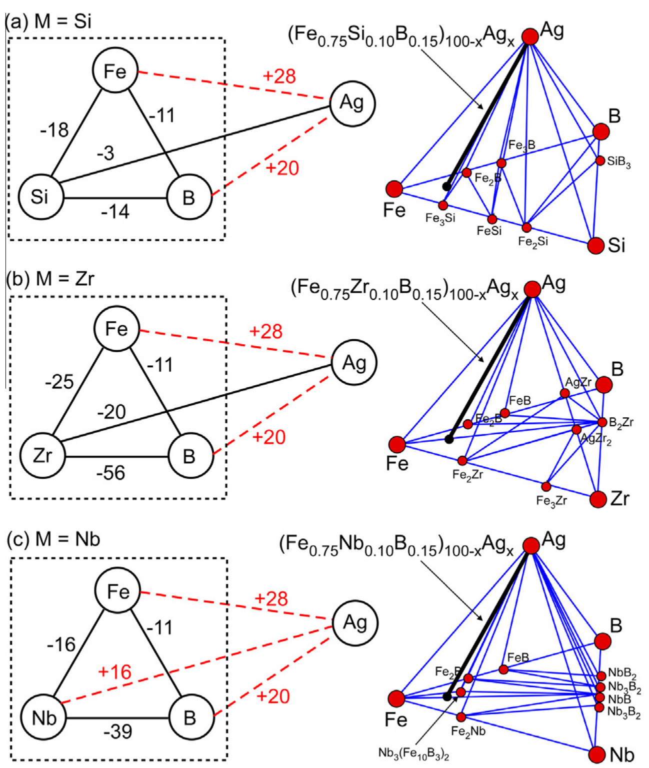

Fig. 2. Prediction method for Fe–Ag-based alloys that exhibit amorphous phase formation and liquid phase separation simultaneously. The left side is a combination map of ΔH_{mix} for binary atomic pairs of constituent elements in quaternary Fe–Ag-based alloys, whereas the right side corresponds to the predicted Fe–Ag-based quaternary phase diagram by *ab initio* calculations. (a) Fe–Ag–Si–B, (b) Fe–Ag–Zr–B, and (c) Fe–Ag–Nb–B.

Fe–Nb–B–Ag (Fig. 2c) alloy, the large negative values of ΔH_{mix} for Fe–Nb, Fe–B, and Nb–B and large positive values of ΔH_{mix} for Ag–Fe, Ag–Nb, and Ag–B are indicative of liquid phase separation to Fe–Nb–B and Ag liquids. Thus, there is no binary Fe–Ag, Nb–Ag, or B–Ag compounds but rather ternary Fe–Nb–Ag, Fe–B–Ag, and Nb–B–Ag or quaternary Fe–Ag–Nb–B intermetallic compounds. This indicates that the interruption of liquid phase separation to Fe–Nb–B- and Ag-based liquids by the formation of intermetallic compounds during cooling is unlikely to occur in a Fe–Nb–B–Ag alloy system.

In contrast, such an ideal situation cannot be achieved with Fe–Si–B–Ag or Fe–Zr–B–Ag alloy systems. For instance, in the Fe–Si–B–Ag alloy system (Fig. 2a), the ΔH_{mix} value of the Si–Ag pair is both small and negative. Moreover, the large negative value of ΔH_{mix} for the Ag–Zr atomic pair and the formation of a binary Ag–Zr-based intermetallic compound are predicted by the phase diagram of the Fe–Zr–B–Ag alloy system (Fig. 2b). However, despite these exceptions, the phase separation in Fe–M–B–Ag (M = Si, Zr) and the high GFA of Fe–M–B (M = Si, Zr) in Fe–M–B–Ag (M = Si, Zr) are typical of alloy systems.

3. Experimental procedures and thermodynamic calculation details

A master ingot of an $(Fe_{0.75}M_{0.10}B_{0.15})_{100-x}Ag_x$ alloy (M = Si, Zr, Nb) was prepared from a mixture of Fe, Ag, Si, Zr, Nb, B, and an Fe–B pre-alloy by arc melting in a water-cooled Cu hearth under a purified Ar atmosphere. A rapidly quenched ribbon was produced from this master ingot by means of single-roller melt spinning method. For this, a roller surface velocity of approximately 42 m s^{-1} was used with a fused quartz nozzle measuring 14 mm in diameter with an orifice diameter of approximately 1.0 mm. Heating of the master ingot was performed by radio-frequency heating. Amorphous phase formation was evaluated by X-ray diffraction (XRD) using Cu Kα radiation, thermal analysis by differential scanning calorimetry (DSC) at a heating rate of 0.67 K s^{-1}, and electron microscopy. Scanning electron microscopy (SEM)-backscattered electron imaging (BEI) and electron probe microanalysis (EPMA)-wavelength dispersive X-ray spectrometry (WDX) were performed using a JEOL JXA-8800R system. Transmission electron microscopy (TEM) was performed using a Hitachi H-800 system at an acceleration voltage of 200 kV. For TEM observation over a wide area and with thick specimens, high voltage electron microscopy (HVEM) was performed using an ultra-high voltage electron microscope (UHVEM) Hitachi H-3000 system [30] at an acceleration voltage of 2.0 MV. The very high acceleration voltage of UHVEM realizes the thick specimen and wide-area TEM observation [31,32]. Thin films for TEM and HVEM observation were prepared by an ion-thinning method using Gatan's model 691 precision ion-polishing system (PIPS™).

The occurrence of liquid phase separation and the partition of constituent elements into separated liquids are discussed on the basis of thermodynamic calculations using the FactSage (ver. 6.4) computation program and the thermodynamic database for alloy systems from the Scientific Group Thermodata Europe (SGTE) [33].

4. Results

In the cross-sectional images of the arc-melted ingots shown in Fig. 3, a macroscopically phase-separated interface is clearly discernible between the metallic gray-silver and the white-gray regions, regardless of the Ag composition x or the M element in the $(Fe_{0.75}M_{0.10}B_{0.15})_{100-x}Ag_x$ (M = Si, Zr, Nb) alloys. Furthermore, there is a clear tendency for a spherical metallic gray-silver region to be embedded within the white-gray phase in all the alloys. Typical examples of the spherical metallic gray-silver and white-gray phase regions are indicated by the indices A and B in Fig. 3a. These features are typical of the solidification structure created by liquid phase separation. Fig. 4 shows the EPMA analyses of the arc-melted ingot of the $(Fe_{0.75}M_{0.10}B_{0.15})_{70}Ag_{30}$ (M = Si, Zr, Nb) alloys, which clearly show macroscopically phase-separated interfaces. In the BEI image of the Fe–Si–B–Ag alloy (Fig. 4a), the gray and white phases represent Fe-rich and Ag-rich phases, respectively, with Si demonstrating a tendency to concentrate in the Fe-rich phases. The macroscopically phase-separated structure, which is composed of Fe-rich and Ag-rich phases, can also be seen in the Fe–Zr–B–Ag (Fig. 4b) and Fe–Nb–B–Ag (Fig. 4c) alloys. In the Fe–Zr–B–Ag alloy (Fig. 4b), Zr can be seen in both the Fe-rich and Ag-rich phases, whereas B is found only in the Fe-rich region. This inhomogeneous distribution of Zr and B can be explained by the formation of Zr–B and Ag–Zr intermetallic compounds. Both Nb and B are more prevalent in the Fe-rich phase than in the Ag-rich phase, as shown in the Fe–Nb–B–Ag alloy (Fig. 4c). Liquid phase separation into Fe-rich and Ag-rich phases is confirmed by the arc-melted ingots of Fe–M–B–Ag (M = Si, Zr, Nb) alloys to be independent of the M element; however, the partitioning of M and B between the Fe-rich and Ag-rich phases is dependent on the M element.